Journal Pre-proof

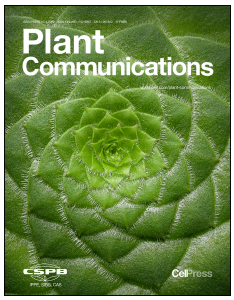

Engineering the hypercompact miniature IscB-ωRNA systems for efficient rice genome editing

Yucai Li, Chenfei Li, Jiaying Yang, Xinrong Sun, Jingying Li, Lei Yan, Chen Zhang, Shaoya Li, Yubing He, Lanqin Xia

PII: S2590-3462(25)00324-4

DOI: https://doi.org/10.1016/j.xplc.2025.101562

Reference: XPLC 101562

To appear in: *Plant Communications*

Received Date: 15 May 2025

Revised Date: 20 August 2025

Accepted Date: 10 October 2025

Please cite this article as: Li, Y., Li, C., Yang, J., Sun, X., Li, J., Yan, L., Zhang, C., Li, S., He, Y., Xia, L., Engineering the hypercompact miniature IscB-ωRNA systems for efficient rice genome editing, *Plant Communications* (2025), doi: https://doi.org/10.1016/j.xplc.2025.101562.

Engineering the hypercompact miniature IscB-ωRNA systems for efficient rice genome editing

Yucai Li [1, 2, †], Chenfei Li [1, 2, †], Jiaying Yang [1], Xinrong Sun [1, 2], Jingying Li [1, 2], Lei Yan [1], Chen Zhang [1], Shaoya Li [1], Yubing He [1, 2, *] and Lanqin Xia [1, 2, *]

[1]State Key Laboratory of Crop Gene Resources and Breeding, Institute of Crop Sciences (ICS), Chinese Academy of Agricultural Sciences (CAAS), Beijing 100081, China

[2] Key Laboratory of Gene Editing Technologies (Hainan), Ministry of Agricultural and Rural Affairs /National Nanfan Research Institute (Sanya), Chinese Academy of Agricultural Sciences, Sanya 572024, Hainan, China

[†] These authors contribute equally to this work.

[*]Corresponding authors: Lanqin Xia (xialanqin@caas.cn) or Yubing He (heyubing@caas.cn)

Running title: Engineered IscB-ωRNA systems for rice gene editing

Dear Editor,

The Insertion Sequences of Cas9-like OrfB (IscB) family, consisting of ~490 residues and as the ancestors of Cas9 endonucleases from IS200/605 transposon, hold great potential for efficient delivery via viral vectors in genome editing of both mammalian cells and plants due to their smaller size (Altae-Tran et al., 2021; Schuler et al., 2022; Han et al., 2023; Han et al., 2024; Xue et al., 2024; Yan et al., 2024). The IscB associates with its cognate 222-nt RNA obligate mobile element-guided activity RNA (ωRNA) along with the transposon-associated motif (TAM) of NWRRNA (N=A/G/C/T, W=A/T, R=A/G) for programmable DNA double strand (DSB) cleavage (Figure 1A) (Altae-Tran et al., 2021; Schuler et al., 2022). Unfortunately, the activity of IscB in mammalian cells is very low, with OgeuIscB only induces indels of less than 5% in HEK293T cells (Altae-Tran et al., 2021). Recent engineered enIscB and/or enωRNA systems through rational design achieved an average 4.3- to 30.4-fold increase in editing efficiency compared to the wild-type IscB/ωRNA, with the highest efficiency reaching up to 91.3% in mammalian cells (Figure 1B, 1C, S1, S2) (Han et al., 2023, 2024; Xue et al., 2024; Yan et al., 2024). Initial assessment of enIscBv1-ωRNA for genome editing in rice protoplasts revealed its relatively lower editing efficiency (Zhang et al., 2024). Whether these different enhanced versions or combinations of enIscB-enωRNA could enable efficient and heritable genome editing in plants remains to be explored. In this study, we systemically investigated the editing performances and outcomes of different combinations of enIscBs and enωRNAs in rice protoplasts. We further fused T5 exonuclease (T5E) to each of these enIscBs at C-terminus (enIscBs-T5E) in order to improve their editing efficacies, respectively. We then tested the performances of these enIscBs-T5E-enωRNAs in rice stable lines in order to facilitate the applications of these miniature enIscB-enωRNA systems in diverse scenarios in plant genome editing.

To systemically test the performances of these different combinations of the optimized enIscBs and enωRNAs at endogenous target sites in rice, we first engineered a series of plant constructs harboring the rice codon optimized enIscBs, respectively (Figure 1D, Table S1, S2). We used a composite 35S promotor to control the

expressions of either ωRNA or the respective enωRNAs (Jiang et al., 2020). We also fused T5E at C-termini of each of the enIscBs to generate five variants with an architecture of enIscB-T5E (Figure 1D, Table S1, S2). Given that IscB or enIscBs produce sticky ends, the fusion of T5E may be an effective strategy for enhancing its editing efficiency (Han et al., 2023; Wang et al., 2025a; Wang et al., 2025b). We first designed ten ωRNAs/enωRNAs targeting eight rice endogenous genes including *OsEP3*, *OsEPFL9-T1*, *OsEPFL9-T2*, *OsFAD*, *OsHd1*, *OsNPT1*, *OsSBEIIb-T1*, *OsSBEIIb-T2*, *OsSLR1*, and *OsSWEET14*, respectively (Table S3). Once these targets are edited, traits of interest could be improved (Table S3). We then tested the effectiveness of these enIscB-enωRNA architectures in rice protoplasts using next-generation sequencing of PCR amplicons. Genotyping results showed that all these enIscB-enωRNA tools exhibited significantly improved editing efficiencies, compared to the IscB-ωRNA (V0) control with which no editing events were detected at several target sites such as *OsEP3*, *OsHd1*, *OsNPT1* and *OsSBEIIb-T1* at all (Figure 1E, Figure S3). Among these enhanced versions, enIscBv1-enωRNAv1 (V1), enIscBv2-enωRNAv2 (V2), enIscBv3-enωRNAv3 (V3), enIscBv3-enωRNAv4 (V4) and enIscBv4-enωRNAv5 (V5) enabled editing efficiencies ranged from 1.32% to 17.33%, 0.56% to 8.96%, 0.56% to 12.55%, 0.82% to 16.79% and 0.45% to 10.67%, with average efficiencies of 3.70%, 2.24%, 3.16%, 3.35% and 2.23%, respectively (Figure 1E, Figure S3, Table S4), representing 5.86- to 9.73-fold higher than WT IscB-ωRNA, consistence with the previous reports in mammalian cells (Han et al., 2023; Xue et al., 2024; Yan et al., 2024). Notably, V1, V3, and V4 exhibited superior performances over others, with the highest efficiencies reached at 17.33%, 12.55%, and 16.79% at the *OsEPFL9*-T2 target site, respectively (Table S4). It was also worth to note that all the enIscB-enωRNA showed a severe target dependent manner, such as at two targets of *OsEPFL9* (T1 and T2) and two targets of *OsSBEIIb* (T1 and T2) with the same gene context (Figure S3), necessitating the screen for more efficient targets before genome editing by enIscBs-enωRNAs.

Fusion of T5E to the enIscB variants significantly increased the overall average

editing efficiencies at the tested endogenous target sites, respectively (Figure 1E). Whereas IscB-T5E-ωRNA (V0-T5E) enhanced it editing efficiency ranged from 0.53% to 7.64%, with an average efficiency of 1.56%, 4.10-fold higher than IscB-ωRNA (V0), EnIscBv1-T5E-enωRNAv1 (V1-T5E), EnIscBv2-T5E-enωRNAv2 (V2-T5E), EnIscBv3-T5E-enωRNAv3 (V3-T5E), EnIscBv3-T5E-enωRNAv4 (V4-T5E) and EnIscBv4-T5E-enωRNAv5 (V5-T5E) exhibited the editing efficiencies ranging from 2.22% to 20.04%, 1.07% to 13.84%, 1.01% to 18.65%, 1.43% to 23.65% and 0.97% to 15.68%, respectively (Figure 1E, Figure S3 and Table S4). As indicated in Figure S3, V0-T5E significantly increased the editing efficiencies across all the ten tested targets compared to V0. The five enIscB-T5E fusions, V1-T5E to V5-T5E, enabled more robust editing efficiencies at 8, 5, 7, 8, and 5 target sites of the 10 tested target sites in comparison to their non-T5E counterparts, respectively (Figure S3), albeit they did not reach at statistically significant level at some individual target sites (Figure S3), due to data variations in transiently transformed rice protoplasts. Notably, all the five enIscB-T5E fusions demonstrated significantly increased editing efficacies at *OsHd1* and *OsSWEET14* when compared to their non-T5E counterparts, respectively (Figure S3), consistence with the previous reports on enhancement of genome editing performance upon T5E fusion (Han et al., 2023; Wang et al., 2025a; Wang et al., 2025b). Furthermore, among these improved variants, V1-T5E, V3-T5E, and V4-T5E outperformed others and exhibited the highest efficiencies of 24.00%, 18.65%, and 23.65% at the *OsEPFL9*-T2 target site, respectively (Figure S3). However, similar to their non-T5E fusion counterparts, the efficiencies varied among different target sites, further indicating a target-site dependency (Figure 1F). This target-site dependency again highlights the necessity of carefully selecting target sites in practical gene editing experiments.

Furthermore, fusion of T5E to the enIscB variants expanded the editing window and induced both insertions and deletions (indels) with various lengths including larger deletions (Figure 1F, 1G, Figure S4). For example, at three representative target sites including *OsEPFL9*-T2, *OsHd1* and *OsSBEIIb*-T1, whereas IscB-ωRNA exhibited an editing window of 10 to 15 nucleotides (nt), counting the end distal to the TAM as

position 1, the editing windows of enIscB-enωRNA variants mainly occurred between 6- and 20-nt with slightly forward- and backward shifts. The fusion of T5E enlarged the editing windows which predominantly encompassed 1- to 22-nt of the protospacer sequences and TAM (Figure 1F). This broadening of the editing window allows for more versatile targeted editing, providing greater flexibility for saturated mutagenesis in directed evolution through genome editing. In addition, whereas IscB only produced 2-5 base pairs (bp) deletions, fusion of T5E to different enIscB-enωRNA variants induced indels with various lengths and larger deletions compared to their non-T5E counterparts (Figure 1G, Figure S4).

Following the initial assessments of different enIscB-T5E-enωRNA variants in rice protoplasts, we then systemically evaluated their editing performances in rice stable lines by using V0 and V0-T5E as controls. Genotypic analysis revealed that V0 failed to induce any editing events across these 10 endogenous target sites in the rice stable lines, whereas V0-T5E only induced targeted mutagenesis with efficiencies ranging from 0% to 3.42%. In contrast, except for similar severe target-dependency in stable lines as observed in rice protoplasts, the enIscB-T5E-enωRNA variants significantly improve the editing performances. For example, V1-T5E, V2-T5E, V3-T5E, V4-T5E and V5-T5E enabled the average editing efficiencies ranging from 2.22% to 41.87%, 0% to 20.70%, 0% to 41.61%, 0% to 36.25% and 1.33% to 18.66%, with the highest efficiency of each variant was 12.24- (41.78%/3.42%), 6.05- (20.70%/3.42%), 12.16- (41.61%/3.42%), 10.60- (36.25%/3.42%), and 5.46-fold (18.66%/3.42%) increase compared to V0-T5E, respectively (Figure 1H, Table S5). Consistence with our results in rice protoplasts, among these, V1-T5E, V3-T5E, and V4-T5E outperformed others and exhibited the highest average efficiencies of 41.87%, 41.61%, and 36.25% at the *OsHd1* target site, respectively (Figure 1H, Table S5). The representative edited lines of these ten target sites derived from V0-T5E, V1-T5E, V2-T5E, V3-T5E, V4-T5E and V5-T5E exhibited DNA fragment deletions of 3- to 47-bp in rice stable lines, respectively (Figure S5). Furthermore, the edited loci were stably inherited in the subsequent generations following Mendelian genetics, as evidenced by the consistent

presence of the edited alleles in the progeny (Table S6). Especially, evaluations of the agronomic traits of these edited lines demonstrated their potential applications in rice breeding. For example, one stable mutant line of *OsSWEET14*, V1-T5E-6, a line carrying a 47-bp deletion which disrupts the effector-binding element (EBE) recognized by the PXO86's transcription-activator-like effector (TALE) in the promoter region of *OsSWEET14*, exhibited markedly enhanced resistance to rice bacterial blight caused by infection of *Xanthomonas oryzae* pv. *oryzae* (*Xoo*) isolate PXO86 compared to wild-type control (Figure 1I), whereas the other two lines V3-T5E-54 and V5-T5E-15 with deletions not reaching out to the EBE element didn't show any resistance at all, consistence to the previous observation of Oliva et al. (2019). Similarly, the *OsEPFL9*-edited lines displayed a significant reduction in stomatal density, a trait has been reported to be associated with enhanced drought tolerance (Yin et al., 2017) (Figure 1J). However, we also noticed that the editing performances of these enIscB-enωRNAs, even their optimized T5E-fused counterparts, were not as efficient as their respective counterparts in mammalian cells (Han et al., 2023; Xue et al., 2024; Yan et al., 2024), probably due to relatively lower temperature of 28~30°C during rice genome editing.

To evaluate the specificities of V0-T5E, V1-T5E, V2-T5E, V3-T5E, V4-T5E, and V5-T5E in rice stable lines, respectively, we examined the off-target possibility of each on-target site. No off-target effects were found at the putative off-target sites predicted from web site (http://skl.scau.edu.cn/offtarget/) in the tested lines (Table S7), indicating the high specificities of these enIscB-T5E-enωRNA variants in plant genome editing.

In summary, we here engineered several hypercompact miniature enIscB-enωRNA systems for efficient rice genome editing by fusing T5E to the enIscBs, respectively. Systemic evaluations of these enIscB-T5E-enωRNA variants in rice protoplasts indicated that fusion of T5E to each of the enIscBs enabled more robust editing, enlarged their editing windows, and induced indels and larger deletions, respectively. Among which, enIscBv1-T5E-enωRNAv1, enIscBv3-T5E-enωRNAv3, and enIscBv3-T5E-enωRNAv4 outperformed other variants, achieving the editing efficiency up to 41.87 % in stable rice lines, albeit all of which exhibiting a severe

target-dependency manner. Further efforts will be necessary in order to improve the robustness of these three hypercompact enIscB-T5E-enωRNA variants and achieve more robust performance across diverse target sites for crop improvement.

SUPPLEMENTAL INFORMATION

Supplemental information is available in the online version of this article.

COMPETING INTERESTS

All the authors declare no competing financial interests.

AUTHOR CONTRIBUTIONS

LX and YH conceived the project. YL, CL, JY, XS, JL, LY, CZ and SL performed the experiments. YH and YL wrote the manuscript. LX revised the manuscript. All the authors read the final version of this manuscript.

ACKNOWLEDGMENTS

We apologize to those whose work we were unable to cite due to space and reference limitations. We thank Associate Professor Zhiyuan Ji and Dr. Jianan Wu, Institute of Crop Sciences, CAAS for their assistances with rice bacterial blight resistance assay and SEM analysis, respectively. This work is partly funded by the National Natural Science Foundation of China (grant No. 32188102 to L.X.), the Biological Breeding-Major Projects (2023ZD04074 to S.L), and the Nanfan Special Project of CAAS (Grant No. YBXM2405, YBXM2406, YBXM2446, YBXM2504 and YBXM2505 to L.X. and Y.H.).

REFERENCES

Altae-Tran, H., Kannan, S., Demircioglu, F.E., Oshiro, R., Nety, S.P., McKay, L.J., Dlakic, M., Inskeep, W.P., Makarova, K.S., Macrae, R.K., et al. (2021). The widespread IS200/IS605 transposon family encodes diverse programmable RNA-guided endonucleases. Science **374**:57-65.

Han, D.Y., Xiao, Q.Q., Wang, Y.F., Zhang, H.A., Dong, X., Li, G.L., Kong, X.F., Wang, S.H., Song, J.H., Zhang, W.H., et al. (2023). Development of miniature base editors using engineered IscB nickase. Nat Methods **20**:1029-1036.

Jiang, Y.Y., Chai, Y.P., Lu, M.H., Han, X.L., Lin, Q.P., Zhang, Y., Zhang, Q., Zhou, Y., Wang, X.C., Gao, C.X. and Chen, Q.J. (2020) Prime editing efficiently generates W542L and S621I double mutations in two ALS genes in maize. Genome Biol. **21**, 257.

Han, L., Hu, Y., Mo, Q., Yang, H., Gu, F., Bai, F., Sun, Y., and Ma, H. (2024). Engineering miniature IscB nickase for robust base editing with broad targeting range. Nat Chem Biol **20**:1629-1639.

Oliva, R., Ji, C., Atienza-Grande, G., Huguet-Tapia, J.C., Perez-Quintero, A., Li, T., Eom, J.S., Li, C., Nguyen, H., Liu, B., et al. (2019). Broad-spectrum resistance to bacterial blight in rice using genome editing. Nat Biotechnol **37**:1344-1350.

Schuler, G., Hu, C., and Ke, A. (2022). Structural basis for RNA-guided DNA cleavage by IscB-omegaRNA and mechanistic comparison with Cas9. Science **376**:1476-1481.

Wang, W., Yan, L., Li, J., Zhang, C., He, Y., Li, S., and Xia, L. (2025a). Engineering a robust Cas12i3 variant-mediated wheat genome editing system. Plant Biotechnol J **23**:860-873.

Wang, W., Li, S., Yang, J., Li, J., Yan, L., Zhang, C., He, Y., and Xia, L. (2025b). Exploiting the efficient Exo:Cas12i3-5M fusions for robust single and multiplex gene editing in rice. J Integr Plant Biol **67 (5)**: 1246-1253.

Xue, N., Hong, D., Zhang, D., Wang, Q., Zhang, S., Yang, L., Chen, X., Li, Y., Han, H., Hu, C., et al. (2024). Engineering IscB to develop highly efficient miniature editing tools in mammalian cells and embryos. Mol Cell **84**:3128-3140.

Yan, H., Tan, X., Zou, S., Sun, Y., Ke, A., and Tang, W. (2024). Assessing and engineering the IscB-omegaRNA system for programmed genome editing. Nat Chem Biol **20**:1617-1628.

Yin, X., Biswal, A.K., Dionora, J., Perdigon, K.M., Balahadia, C.P., Mazumdar, S., Chater, C., Lin, H.C., Coe, R.A., Kretzschmar, T., et al. (2017). CRISPR-Cas9 and CRISPR-Cpf1 mediated targeting of a stomatal developmental gene EPFL9 in rice. Plant Cell Rep **36**:745-757.

Zhang, R., Tang, X., He, Y., Li, Y., Wang, W., Wang, Y., Wang, D., Zheng, X., Qi, Y., and Zhang, Y. (2024). IsDge10 is a hypercompact TnpB nuclease that confers efficient genome editing in rice. Plant Commun **5**:101068.

FIGURE LEGENDS

Figure 1. Schematic diagrams of different enIscB-enωRNA variants and their editing outcomes in rice protoplasts and stable transgenic rice lines, respectively.

(**A**) (**i**), The predicted structure of the IscB-ωRNA-target DNA ternary complex. IscB is in green, ωRNA is in yellow, target strand is in red, and non-target strand is in blue. (**ii**), Domain organization of IscB. P1D, P1 interaction domain; TID, TAM-interaction domain. RuvC domain is separated into three segments: RuvC I, RuvC II, and RuvC III. (**iii**), Schematic diagrams illustrate the gene editing process mediated by IscB. TAM, transposon-associated motif, TS, target strand, NTS, non-target strand, DSB, double strand break, NHEJ means nonhomologous end joining, indels, insertion and deletions.

(**B**) The native IscB and four enIscB variants developed by rational design (Altae-Tran et al., 2021; Han et al., 2023; Han et al., 2024; Xue et al., 2024; Yan et al., 2024).

(**C**) (**i**), Secondary structure of ωRNA according to the crystal structure of IscB-ωRNA (Han et al., 2023). (**ii**), The native ωRNA and different versions of optimized ωRNAs (enωRNAs) (Altae-Tran et al., 2021; Han et al., 2023; Han et al., 2024; Xue et al., 2024; Yan et al., 2024).

(**D**) Schematic diagrams of IscB-ωRNA (V0), IscB-T5E-ωRNA (V0-T5E), enIscBv1-enωRNAv1 (V1), enIscBv1-T5E-enωRNAv1 (V1-T5E), enIscBv2-enωRNAv2 (V2), enIscBv2-T5E-enωRNAv2 (V2-T5E), enIscBv3-enωRNAv3 (V3), enIscBv3-T5E-enωRNAv3 (V3-T5E), enIscBv3-enωRNAv4 (V4), enIscBv3-T5E-enωRNAv4 (V4-T5E), enIscBv4-enωRNAv5 (V5), and enIscBv4-T5E-enωRNAv5 (V5-T5E). The IscB and its enIscB variants are driven by a maize *Ubiquitin* promotor (*Ubi*). The enωRNA variants are expressed under the control of the 35S-CmYLCV-U6 composite promoter and terminated with 'TTTTTTT'. The *hpt* is used as a selection marker gene. T5E, T5 Exonuclease.

(**E**) Frequencies of targeted genome editing by V0, V0-T5E, V1, V1-T5E, V2, V2-T5E, V3, V3-T5E, V4, V4-T5E, V5, and V5-T5E at ten target sites in protoplasts. Each data point corresponds to an independent event. Different letters indicate significant differences, determined using a one-way ANOVA ($P < 0.05$; Duncan test).

(**F**) The editing windows of different versions of enIscB-enωRNAs at the *OsEPFL9*-T2, *OsHd1* and *OsSBEIIb*-T1 endogenous target sites in rice protoplasts.

(**G**) The profiles of deletion size induced by various versions of enIscB-enωRNAs at the *OsEPFL9*-T2, *OsHd1* and *OsSBEIIb*-T1 endogenous target sites in rice protoplasts.

(**H**) The performances of different enIscB-T5E-enωRNAs in rice independent transgenic lines, respectively. The editing efficiencies are calculated based on three independent biological replicates (each replicate was performed with 3 repeats). Different letters indicate significant differences, determined by using a one-way ANOVA ($P < 0.05$; Duncan test).

(**I**) (**i**), The mutation patterns in *OsSWEET14* promoter were derived from V1-T5E, V3-T5E and V5-T5E in the T_2 lines, respectively. The PAM sequences are highlighted in purple. The target sequence is underlined. The effector-binding element (EBE) recognized by transcription-activator-like effector (TALE) of the *Xoo* isolate PXO86 in the *OsSWEET14* promoter is enclosed in the dashed box. The dashed lines indicate nucleotide deletions. (**ii**), The morphology of wild-type ZH11 and *OsSWEET14*-edited lines before and 14 d after inoculation with PXO86. Scale bar, 20 cm. (**iii**), Phenotypes of leaves from 8-week-old ZH11 wild-type and *OsSWEET14* promoter-edited mutant plants inoculated with the PXO86. Scale bar, 2 cm. (**iv**), Lesion lengths on PXO86-inoculated leaves were measured 14 d post-infection. Data are means ± SD of three independent plants (three to six leaves per plant). ZH11, wild-type Zhonghua11; V1-T5E-6, V3-T5E-54, and V5-T5E-15: T2 lines harboring 47-, 9-, and 4-bp promoter deletions, respectively. Only 47-bp deletion disrupts the EBE recognized by the PXO86's TALE in the *OsSWEET14* promoter. Different letters indicate significant differences, determined by using a one-way ANOVA ($P < 0.05$; Duncan test).

(**J**) (**i**), Scanning electron micrographs of stomatal distribution in wild-type (ZH11) and *OsEPFL9* mutants. Representative stomata are indicated by white arrows. A close-up view of stomata are shown in the upper-right corner of the images. Scale bar, 50 μm. (**ii**), Stomatal density was quantified in wild-type ZH11 and the T2 mutant line of V1-T5E-17, which harbors a 7-bp in-frame deletion within the *OsEPFL9* coding region, respectively. V1-T5E-17 exhibited significantly lower stomatal density than the wild-type control. Different letters indicate significant differences, determined by using Student's two-tailed unpaired t-test ($P < 0.05$).

A

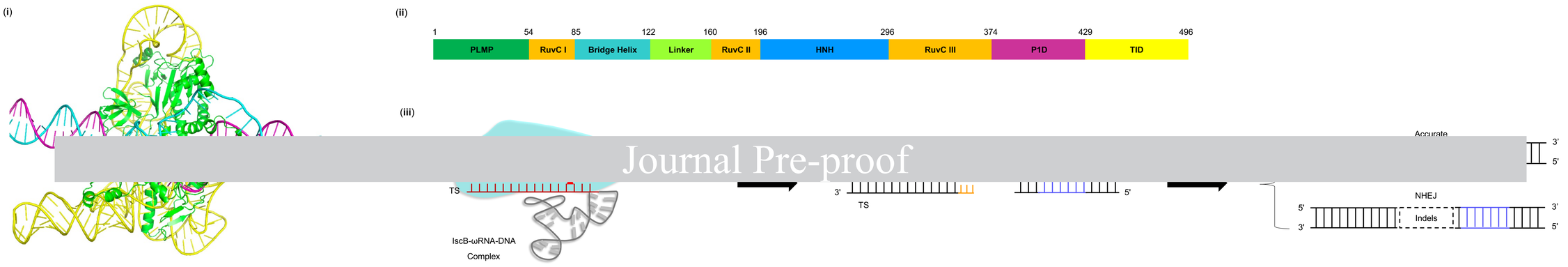

B

IscB variants	Lengths	Amino acid mutations	Ref
IscB	496 aa		Altae-Tran et al., 2021
enIscBv1	496 aa	E85R, H369R, S387R, S457R	Han et al., 2023
enIscBv2	496 aa	E84R, D96R, K118R	Xue et al., 2024
enIscBv3	496 aa	M102R, F137K, V159K, N281R, Q324R, Y327K, H368R, L393K	Yan et al., 2024
enIscBv4	496 aa	D97K, F138N, S431K, S457R	Han et al., 2024

C

(i)

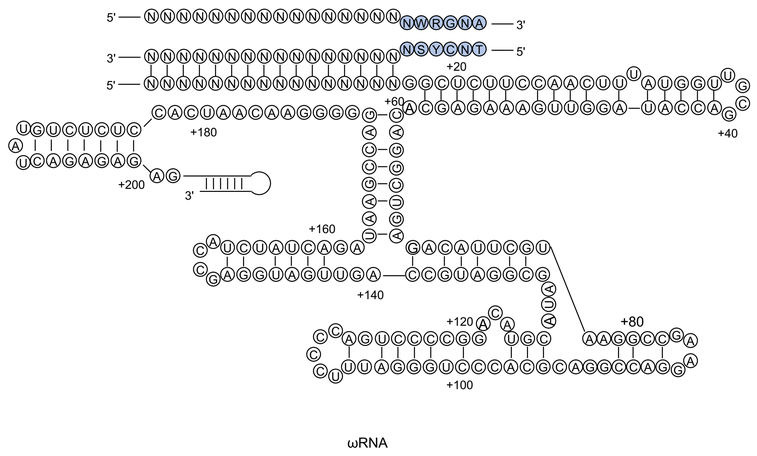

(ii)

ωRNA variants	Lengths	Redesigned ωRNAs	Ref
ωRNA	222 nt		Altae-Tran et al., 2021
enωRNAv1	207 nt	$rU^{+6}>rG^{+6}$, $\Delta rU^{+13}\sim rG^{+31}$, $rU^{+38}>rC^{+38}$, $rG^{+70}>rA^{+70}$, $rA^{+72}>rG^{+72}$, $rC^{+107}>rA^{+107}$, $rA^{+108}>rC^{+108}$, $rC^{+136}>rA^{+136}$	Han et al., 2023
enωRNAv2	181 nt	$\Delta rU^{+13}\sim rG^{+31}$, $rA^{+11}>rG^{+11}$, $\Delta rC^{+65}\sim rA^{+72}$, $rC^{+103}>rA^{+103}$, $\Delta rG^{+174}\sim rU^{+177}$	Xue et al., 2024
enωRNAv3	186 nt	$rC^{+8}>ru^{+8}$, $\Delta rU^{+15}\sim rU^{+29}$, $rG^{+70}>rA^{+70}$, $rA^{+72}>rG^{+72}$, $rC^{+107}>rA^{+107}$, $rA^{+108}>rC^{+108}$, $rC^{+122}>rU^{+122}$, $rC^{+135}>rA^{+135}$, $rC^{+136}>rA^{+136}$	Yan et al., 2024
enωRNAv4	185 nt	$\Delta rU^{+15}\sim rU^{+29}$, $rG^{+70}>rA^{+70}$, $rA^{+72}>rG^{+72}$, $rC^{+107}>rA^{+107}$, $rA^{+108}>rC^{+108}$, $rC^{+122}>rU^{+122}$, $rC^{+135}>rA^{+135}$, $rC^{+136}>rA^{+136}$	Yan et al., 2024
enωRNAv5	202 nt	$\Delta rU^{+15}\sim rU^{+29}$, $rG^{+70}>rA^{+70}$, $rC^{+107}>rA^{+107}$, $rA^{+108}>rC^{+108}$, $rC^{+136}>rA^{+136}$	Han et al., 2024

D

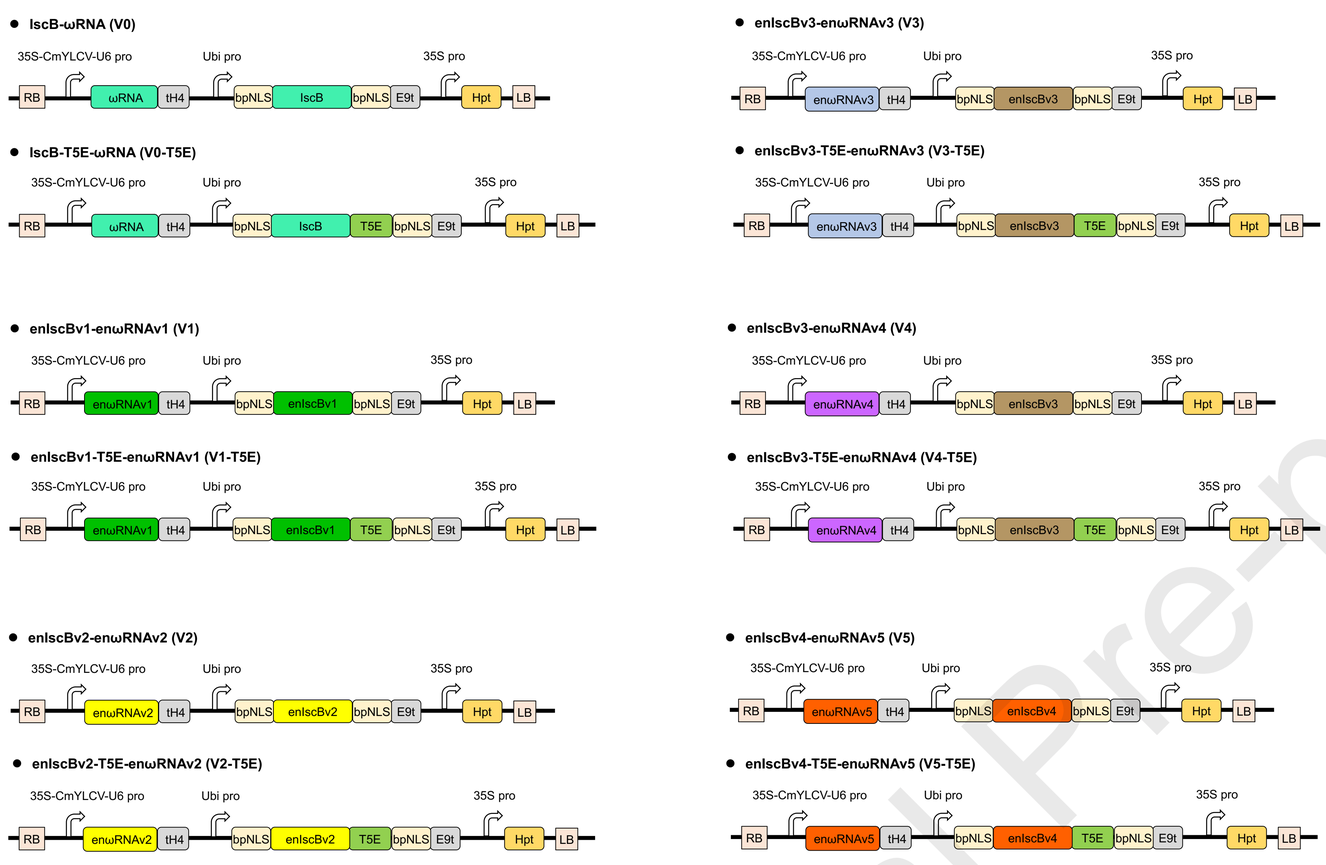

E

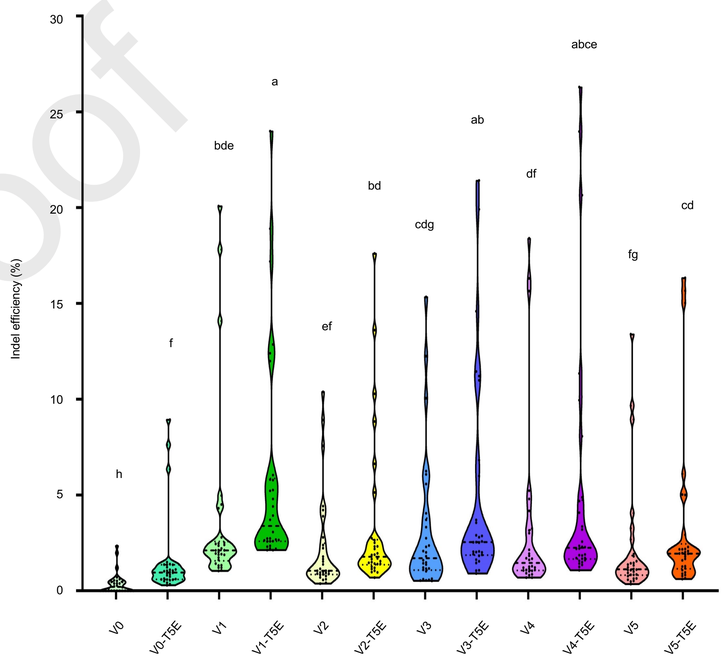

F

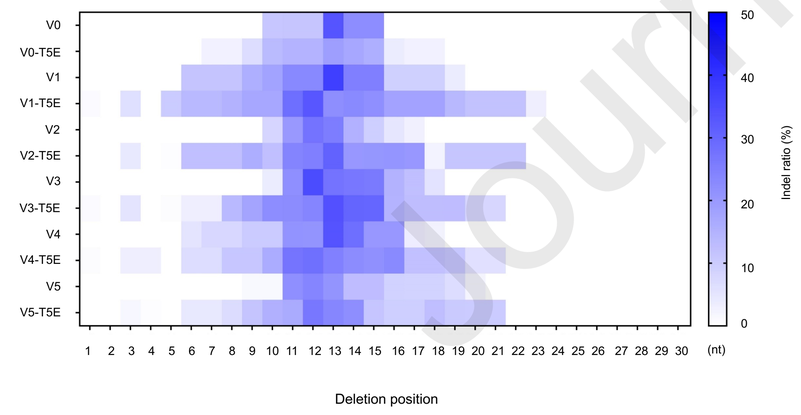

G

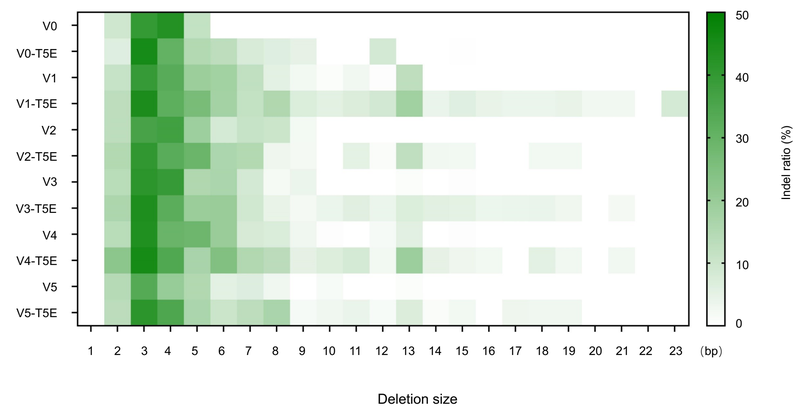

H

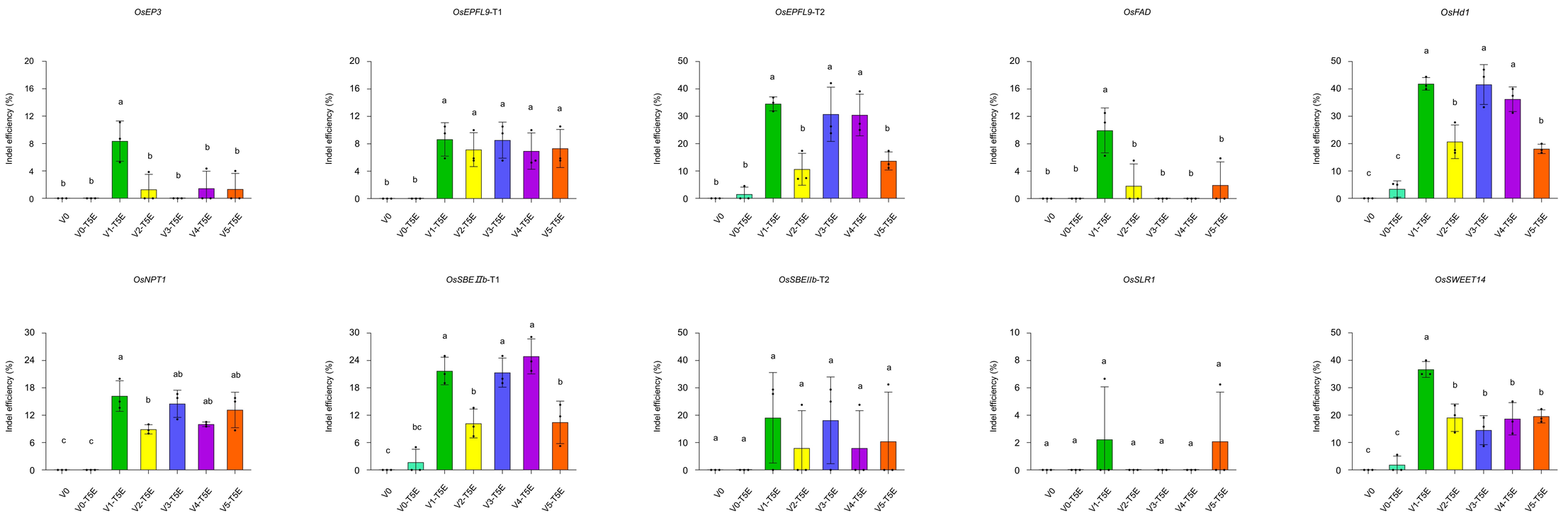

I

(i)

```
OsSWEET14 WT    TAGCACTATATAAACCCCCTCCAACCAGGTGCTAAGCTCATCAAGCCTTCAAGCAAAGCAAACTCAAGTAGTAGCTGAT
                    EBE
V1-T5E-6        TAGCACTATATAAA----------------------------------------------ACTCAAGTAGTAGCTGAT   -47 bp
V3-T5E-54       TAGCACTATATAAACCCCCTCCAACCAGGTGCTAAGC---------CTTCAAGCAAAGCAAACTCAAGTAGTAGCTGAT   -9 bp
V5-T5E-15       TAGCACTATATAAACCCCCTCCAACCAGGTGCTAAGCT----AAGCCTTCAAGCAAAGCAAACTCAAGTAGTAGCTGAT   -4 bp
```

(ii)

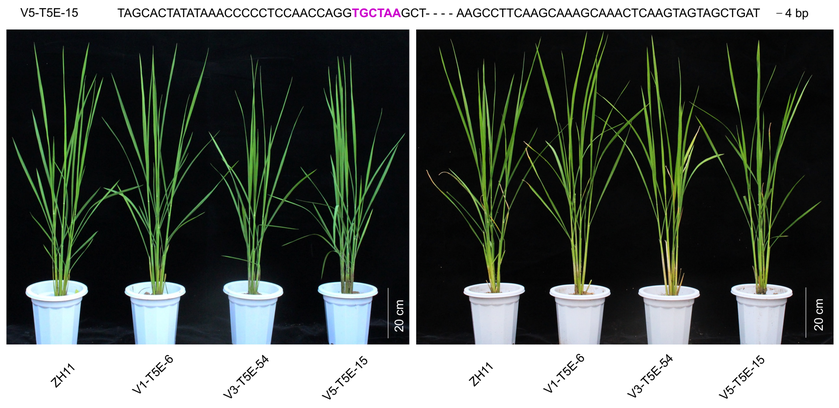

(iii)

(iv)

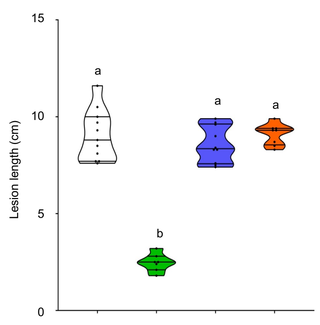

J

(i)

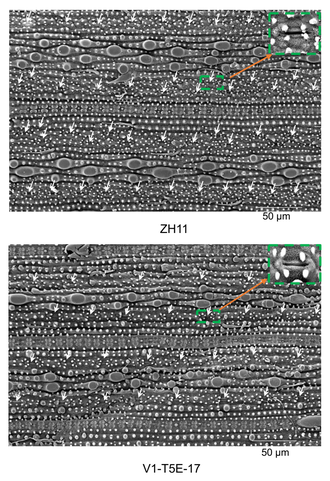

(ii)